Climate Risk Management 2 (2014) 26–41

Contents lists available at ScienceDirect

Climate Risk Management

journal homepage: www.elsevier.com/locate/crm

A geospatial dataset for U.S. hurricane storm surge and sea-level rise vulnerability: Development and case study applications

Megan C. Maloney, Benjamin L. Preston *

Climate Change Science Institute and Environmental Sciences Division, Oak Ridge National Laboratory, PO Box 2008, One Bethel Valley Road, Oak Ridge, TN 37831-6253, United States

ARTICLE INFO

Article history:
Available online 28 February 2014

Keywords:
Climate change
Storm surge
Hurricane
Sea-level rise
Coastal vulnerability
Exposure

ABSTRACT

The consequences of future sea-level rise for coastal communities are a priority concern arising from anthropogenic climate change. Here, previously published methods are scaled up in order to undertake a first pass assessment of exposure to hurricane storm surge and sea-level rise for the U.S. Gulf of Mexico and Atlantic coasts. Sea-level rise scenarios ranging from +0.50 to +0.82 m by 2100 increased estimates of the area exposed to inundation by 4–13% and 7–20%, respectively, among different Saffir-Simpson hurricane intensity categories. Potential applications of these hazard layers for vulnerability assessment are demonstrated with two contrasting case studies: potential exposure of current energy infrastructure in the U.S. Southeast and exposure of current and future housing along both the Gulf and Atlantic Coasts. Estimates of the number of Southeast electricity generation facilities potentially exposed to hurricane storm surge ranged from 69 to 291 for category 1 and category 5 storms, respectively. Sea-level rise increased the number of exposed facilities by 6–60%, depending on the sea-level rise scenario and the intensity of the hurricane under consideration. Meanwhile, estimates of the number of housing units currently exposed to hurricane storm surge ranged from 4.1 to 9.4 million for category 1 and category 4 storms, respectively, while exposure for category 5 storms was estimated at 7.1 million due to the absence of landfalling category 5 hurricanes in the New England region. Housing exposure was projected to increase 83–230% by 2100 among different sea-level rise and housing scenarios, with the majority of this increase attributed to future housing development. These case studies highlight the utility of geospatial hazard information for national-scale coastal exposure or vulnerability assessment as well as the importance of future socioeconomic development in the assessment of coastal vulnerability.

Introduction

Enhancing understanding of the implications of climate variability and change for coastal assets and communities is a high priority for researchers as well as coastal managers (Klein and Nicholls, 1999; Preston et al., 2011). Over the past decade, natural disasters at disparate points along the U.S. coast including Hurricanes Sandy, Katrina, and Irene have contributed billions of dollars in direct and indirect economic losses, displaced millions, and caused significant morbidity and mortality. Such discrete events, as well as a general upward trend in U.S. disaster losses (Van Der Vink et al., 1998; Cutter and Emrich,

* Corresponding author. Tel.: +1 865 456 6531; fax: +1 865 574 9501.
E-mail address: prestonbl@ornl.gov (B.L. Preston).

http://dx.doi.org/10.1016/j.crm.2014.02.004
2212-0963

2005; Gall et al., 2011), have highlighted the vulnerability of the U.S. coastal population and built environment to extreme weather events (Gall et al., 2011; Preston, 2013). Nevertheless, various driving forces will interact to further increase such vulnerability in coming decades (Preston et al., 2013). Anthropogenic climate change is projected to increase the intensity of future tropical cyclones due to its effect on higher sea surface temperatures (Mendelsohn et al., 2012). Meanwhile, those higher ocean temperatures are projected to increase global sea level. Yet, human decision-making regarding the development of coastal areas and disaster risk management is also likely to contribute to future vulnerability (Pielke, 1860; Titus et al., 2009; Gall et al., 2011; Mendelsohn et al., 2012; Preston, 2013). For example, Mendelsohn et al. (2012) and Preston (2013) project U.S. hurricane losses will increase several fold over the 21st century due to continued development along the Gulf of Mexico and Atlantic coasts. Although historical evidence suggests the United States has made incremental improvements to increase societal resilience to hurricanes (Changnon and Easterling, 2000; Cigler, 2009; Gurley and Masters, 2011), such incremental change does not appear to have been sufficient to offset the rate of growth in societal exposure (Gall et al., 2011; Preston, 2013). To the contrary, Titus et al. (2009) demonstrate that local governments along the U.S. Atlantic Coast intend to develop the majority of coastal lands below 1 m in elevation, despite increasing awareness of sea-level rise, not to mention historical experience with hurricanes.

In light of these trends, recent years have witnessed rapid growth in coastal vulnerability assessments, both in the United States and internationally (Preston et al., 2011). In particular, geospatial information regarding exposure and vulnerability is seen as a particularly valuable means of supporting risk communication and spatial planning for climate adaptation and disaster risk management (Preston et al., 2011). Yet, different approaches to assessment may be pursued depending on the type of information that is sought by researchers and stakeholders and the level of investment that is required. Sharples et al. (2008), for example, propose a three-tiered approach to iterative coastal risk assessment ranging from a national first pass that identifies sensitive coastlines, to a regional second pass that examines vulnerability to physical processes, to a site-specific third pass that evaluates different coastal management options in the context of local geomorphological characteristics and site values. These different approaches to assessment imply potential trade-offs between the scale of the assessment and its robustness with respect to informing subsequent decision-making. That said, rapid advances in geospatial data and computational processing tools for their analysis over the past decade has greatly enhanced the capacity to undertake assessments over expansive geographic scales while still capturing spatially explicit physical processes and characteristics of coastlines.

Even within the aforementioned typology of assessment approaches, different tools and methods may be employed to capture various processes that are deemed important for understanding vulnerability (Voice et al., 2006; McLeod et al., 2010). For example, a range of studies focus on storm surge and the influence of future sea-level rise on return intervals for surges of a given magnitude (Lowe and Gregory, 2005; Claudia et al., 2012; Lin et al., 2012; Grinsted et al., 2013). However, such studies do not propagate those surges over land, and thus the consequences of changes in return frequency for inundation and societal losses go unaddressed. One common approach for understanding the exposure of coastal areas to inundation has been simply to compare coastal elevation contours with different scenarios of sea-level rise (Nicholls et al., 1999; Titus and Richman, 2001; Nicholls and Small, 2002; DCC, 2009; Nicholls et al., 2010; Nicholls and Cazenave, 2010; Tebaldi et al., 2012). Such studies, however, often do not account for the routing of water across the landscape and thus are largely representations of the relative low-lying nature of coastal lands. Moreover, although sea-level rise has been affecting the U.S. coast for the past century (Aubrey and Emery, 1983; Roemmich, 1992; Nicholls and Leatherman, 1996; Gehrels et al., 2002; Church et al., 2004; Kemp et al., 2011; Houston and Dean, 2011), significant loss and damage has largely been associated with acute events such as hurricanes and the associated wind, wave, and storm surge damage. This suggests the need to integrate sea-level rise and storm surge for meaningful assessment of the physical vulnerability of the coast (Rygel et al., 2006; Kleinosky et al., 2007; Frazier et al., 2010; Mahendra et al., 2011; Gilmer et al., 2012; McInnes et al., 2013). Yet, such studies are commonly confined to discrete regions due to the needs of the project, availability of required data, and/or the time-intensive nature of such modeling (McLeod et al., 2010). As a consequence, there are few examples of the application of such approaches over large geographic areas (Hoffman et al., 2010). National assessments of coastal vulnerability, for example, are often based upon simple analyses of elevation contours (DCC, 2009), reflecting potential inundation of coastal land areas due to sea-level rise, or the development of vulnerability indices based upon relevant physical variables (Hammar-Klose and Thieler, 2001; Boruff et al., 2005; Gutierrez et al., 2011; Yin et al., 2012).

The objective of the current study was to scale-up previously published methods for the integrated assessment of coastal vulnerability to hurricane storm surge and sea-level rise (Rygel et al., 2006; Kleinosky et al., 2007; Frazier et al., 2010) to develop contiguous, process-based, geospatial inundation layers for the U.S. coastlines of the Gulf of Mexico and the Atlantic Ocean. These data are then used to explore geographic variability in exposure of U.S. coastlines to storm surge inundation as well as the relative importance of hurricane intensity and different scenarios regarding future global mean sea-level rise. Furthermore, as a rich body of literature reflects the importance of considering physical vulnerability in the context of social vulnerability (Cutter et al., 2003; Turner et al., 2003a,b; Rygel et al., 2006; Smit and Wandel, 2006; Kleinosky et al., 2007; Füssel, 2007; Preston et al., 2009; Frazier et al., 2010; Preston et al., 2011), two case studies are used to illustrate applications of these geospatial data for first pass assessments of the exposure of societal assets. The first focuses on U.S. energy infrastructure in the Southeast, and the second focuses on residential housing for both the Gulf and Atlantic coasts. The subsequent discussion synthesizes cross-cutting insights that emerge from these case study applications regarding challenges and opportunities for using hazard data for such assessment activities.

Methods

Development of geospatial storm surge hazard layers

The geographic distribution of storm surge hazard zones was delineated using archived simulations with the Sea, Lake and Overland Surges from Hurricanes (SLOSH) model from the National Hurricane Center (NHC) of the National Oceanic and Atmospheric Association (NOAA) (NWS, 2011). The SLOSH model estimates storm surge heights associated with hurricanes by simulating the effects of storm size, forward speed, track, wind speed and atmospheric pressure on water heights in the coastal zone. Data products from the SLOSH model are available for 37 basins along the coasts of the Atlantic Ocean, Gulf of Mexico, Caribbean Sea, and Hawaii that are exposed to hurricanes, including population centers, ports, or low-lying topography where the effects of storm surge are greatest (NWS, 2011; Burkett and Davidson, 2012). SLOSH basins consists of a grid definition as well as various geographic features that route and impede the flow of water. Storm surge within a basin can be represented using a polar, elliptical, or hyperbolic grid with a variable resolution, with the higher resolutions associated with the area of interest. For example, the grid used in the current study for the New Orleans basin had a horizontal resolution of approximately 6.9 km at its furthest point offshore (approximately 300 km), 1.6 km over downtown New Orleans, and 0.6 km at its most inland point.

Storm surge modeling with SLOSH can be approached in three ways: a deterministic model that predicts a single event based on inputs and assumes perfect information; a probabilistic model that creates a suite of runs for specific storm input and incorporates past forecasts' statistical errors into its analysis; and a composite model that relies on a range of variables and combination of runs. The archived data products from the composite approach best fit our need to assess potential exposure to a range of future storms over a centennial time scale. For the composite model, the NHC performed hurricane simulations for each basin for the five Saffir-Simpson categories using varying forward speeds, landfall directions, and landfall locations (Frazier et al., 2010). Several thousand hurricane simulations were run for each basin; for example, 1640 hypothetical hurricanes were modeled for the New Orleans basin (FEMA et al., 2003). Model simulations generate values for the maximum storm surge surface water elevation obtained in each grid cell, called Maximum Envelopes of Water (MEOWs) (Rygel et al., 2006; Kleinosky et al., 2007; Frazier et al., 2010). The MEOWs for each basin form a composite dataset called Maximum of MEOWS (MOMs) (Rygel et al., 2006; Kleinosky et al., 2007; Frazier et al., 2010). The MOMs represent the spatial distribution of potential storm surge elevation for a particular category of tropical cyclone at a particular tide (NWS, 2011). For storm surge heights of individual hurricanes, this model is accurate to within ±20% (NWS, 2011).

For the current study, data from 33 of the 37 SLOSH basins corresponding to the Gulf and Atlantic coasts were selected as focal areas. In order to convert SLOSH MOM grids into inundation layers, the storm surge surface water elevations associated with MOM grids for each basin were compared with the underlying land elevation. The MOM grids for high tide were used in order to capture inundation risk associated with tidal variability. For each basin, MOM grids representing high tide were converted to points using the geographic information system software ArcMAP 10 from ESRI. Points containing no storm surge information were interpreted as dry points and deleted, leaving only points with a non-zero storm surge estimate. A second-order inverse distance-weighting algorithm was subsequently applied to the remaining points to generate a smoothed inundation surface at 30 m resolution. The MOM values represented surface water elevation above the datum, including topography, but the coarse resolution of the SLOSH modeling domain results in poor representation of land surface elevation. Hence, this storm surge elevation layer was subsequently compared against a composite grid of USGS 1 arc-second (~30 m horizontal resolution) National Elevation Dataset (NED) tiles corresponding with the spatial extent of the MOM. The NED is a composite of best available elevation data for the U.S. assembled by the USGS (Gesch et al., 2002; Gesch, 2007). However, the vertical accuracy of NED expressed as a root mean square error is estimated at 2.44 m (Gesch, 2007). Hence, caution is warranted in using NED as a basis for making judgments about potential inundation or water depth (Murdukhayeva et al., 2013). Land elevations were subtracted from the interpolated storm surge surface, resulting in a surface indicating depth of water above land. Due to the various uncertainties associated with SLOSH and the NED data, inundation grids were converted to binary values by ranking positive depth values as 1, wet, and zero values as 0, dry. Cells with 0 values were subsequently deleted as these represented locations where the estimated storm surge elevation was below the land surface elevation and thus unlikely to be inundated. The remaining wet cells were converted to a polygonal hazard zone delineating the spatial distribution of coastal areas within a basin that is potentially exposed to storm surge from a hurricane of a given Saffir-Simpson classification. This process was repeated for each of the 33 basins included in the current study. As storm surge estimates for a subset of basins were generated using the older National Geodetic Vertical datum 1929 (NGVD29), MOMs for those basins were converted to the North American Vertical datum of 1988 (NAVD88) to maintain consistent datum assumptions among basins as well as with elevation data. This was done by applying the data transformation grid files associated with the VERTCON 2.0 datum conversion model developed by the National Geodetic Survey to convert MOM layers from basins using NGVD 29. The transformation files are raster files containing a conversion factor for translating NGVD29 elevations into NGVD88 elevations (Young, 2003). Once hazard polygons were generated for all 33 basins, they were amalgamated into a seamless data layer spanning the entire U.S. coastline from Texas to Maine. However, state and county administrative boundaries were maintained to enable data aggregation, integration, and analysis at these levels geopolitical levels.

Incorporation of sea-level rise

In addition to the development of storm surge hazard data based upon hurricanes alone, additional data layers were developed to represent the effects of sea-level rise on future storm surge inundation. Significant uncertainty is associated with estimates of future sea-level rise over the 21st century, and particular differences are observed between model based-estimates and empirical approaches, which tend to yield higher magnitudes of sea-level rise (Rahmstorf, 2007; Meehl et al., 2007; Pfeffer et al., 2008; Hunter, 2010; Rahmstorf, 2010; Rahmstorf et al., 2012). Much of the impact assessment literature over the past decade has used the *Special Report on Emissions Scenarios* (Nakicenovic et al., 2000) as a guide for both future greenhouse gas emissions as well as future socioeconomic conditions (Bierwagen et al., 2010) in recognition of the fact that climate change will manifest in concert with changing social, economic, and political contexts. Therefore, the sea-level rise values used for our calculations were developed by Hunter (Hunter, 2010), who reconciled projections from the IPCC Fourth Assessment Report (AR4) with the sea-level rise time series of the IPCC's *Third Assessment Report* to better account for the additional contributions of ice sheet discharge (IPCC, 2001; Hunter, 2010). Sea-level rise projections by 2100 from four of the illustrative SRES scenarios were used: A1Fi (+0.82 m), A2 (+0.69 m), B1 (+0.50 m) and B2 (+0.58 m) as well as fifth (base case) that represented no sea-level rise. Although based upon scenarios originally published in 2001 (IPCC, 2001), these sea-level rise estimates are consistent with those of the more recent AR5 report (IPCC, 2013). For example, the AR5 upper estimate of likely global sea-level rise in 2100 associated with representative concentration pathway (RCP) 8.5 is also 0.82 m (IPCC, 2013), although other RCPs generate sea-level rise estimates by 2100 that are as low as 0.26 m.

These sea-level rise assumptions were incorporated by adding the respective sea-level rise scenarios to the interpolated storm surge surface prior to their conversion to binary values. No assumption was made with respect to the absolute or relative likelihood of the different sea-level rise scenarios, and the position of the shoreline was not adjusted for sea-level rise inundation, so resulting hazard zones do not separate land inundated by sea level rise from land inundated by storm surge. In addition, while the SLOSH model dynamics account for flow around barriers, our methods did not retain that accuracy when adding sea-level rise. Inundation values were raised regardless of exposure to inflow, which could cause isolated valleys to have positive flood values. To identify these isolated cells, the focal statistics tool was used to determine whether a flooded cell was tangent to another flooded cell that could have exposed it to inflow. Cells that did not touch another flooded cell were considered isolated by elevation barriers and were masked out of further calculations. These methods resulted in five distinct coastal storm surge inundation hazard datasets for each of the five Saffir-Simpson categories, resulting in 25 different hazard layers for the United States, which were archived as ArcGIS shapefiles ranging in size from 129 to 183 megabytes. As the sea-level rise scenarios do not account for transient changes in sea-level between the present and 2100, the resulting hazard layers represented hazard zones that may be exposed to storm surge inundation over the 21st century.

Results

The geospatial hazard layers indicated that approximately 87,000 km^2 of U.S. coastal land area is potentially exposed at present to storm surge inundation from category 1 hurricanes (Figs. 1 and 2). This value is consistent with the 77,612 km^2 estimated to be the land area along the U.S. Atlantic and Gulf Coasts defined by the Federal Emergency Management Agency as being subject to a 1% annual flood probability (Crowell et al., 2010). Although the estimated return interval for category 1 storms along the U.S. coast is much less than 100 years (Keim et al., 2007), differences in the manner in which flood hazard and storm surge hazard are calculated limit the utility of direct comparisons between the hazard metrics (US Army Corps of Engineers et al., 2011). However, the relative exposure of different coastal regions to inundation was consistent with prior studies based on elevation contours (Titus and Richman, 2001). The exposed area increased significantly with the Saffir-Simpson scale, with the area potentially exposed to category 2 storms approximately 28% greater than that for category 1, and the area potentially exposed to category 5 storms almost 84% greater than that for a category 1 storms (Fig. 2). The area exposed to category 5 storms was similar to that for category 4 storms at the national level, because landfalling category 5 storms are extremely rare in the U.S. Northeast, and therefore the NOAA category 5 storm surge dataset coverage did not extend north of Maryland, excluding a large amount of area from our calculations. In fact, since 1900, no storm greater than category 3 has made landfall in the Northeast (Vallee, 2000). However, on a regional or local level in southern latitudes, category 5 events produced storm surge inundation greater than a category 4 storm.

Future sea-level rise increased the area of the U.S. coast that would be inundated by storm surge events (Figs. 1 and 2) (Rygel et al., 2006; Kleinosky et al., 2007; Frazier et al., 2010). On a relative basis, the effects of sea-level rise were more pronounced for lower magnitude storms as the ratio of sea-level rise to storm surge was greater (Fig. 3). For example, for a category 1 storm, the area vulnerable to storm surge inundation increased by 13–20% among the different sea-level rise scenarios. In contrast, for a category 5 storm, the area subject to inundation increased by 4–7%. As the response of inundation to sea-level rise was highly linear, inundation response functions for the SLOSH results were extrapolated to higher levels of sea-level rise using least-squares linear regression, with the sea-level rise scenario for each Saffir-Simpson category as the independent variable and area inundated as the dependent variable (Fig. 2). The r^2 values for regression models for each Saffir-Simpson hurricane category ranged from 0.98 to 1.00 and were significant at the $\alpha < 0.01$ level. Although such extrapolation is only indicative, it suggests that a 2 m increase in sea level by 2100 would increase the area subject to inundation for category 1 storms by approximately 49%, while for category 5 storms the increase would be approximately 20%. Even when

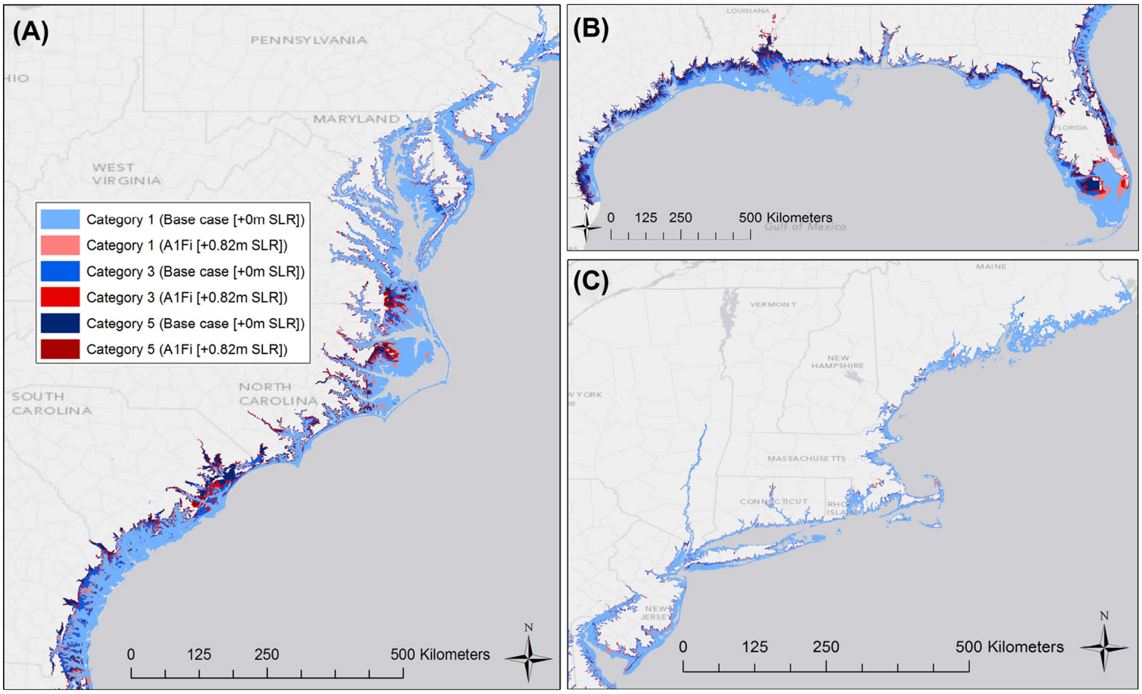

Fig. 1. Contiguous U.S. hurricane storm surge inundation zones for selected Saffir-Simpson categories (1, 3 and 5) assuming no sea-level rise (base case) or the highest sea-level rise modeled in the current study (A1Fi; +0.82 m). The three maps represent three different coastal regions: (A) Gulf of Mexico, (B) Southeast and Mid-Atlantic, and (C) New England.

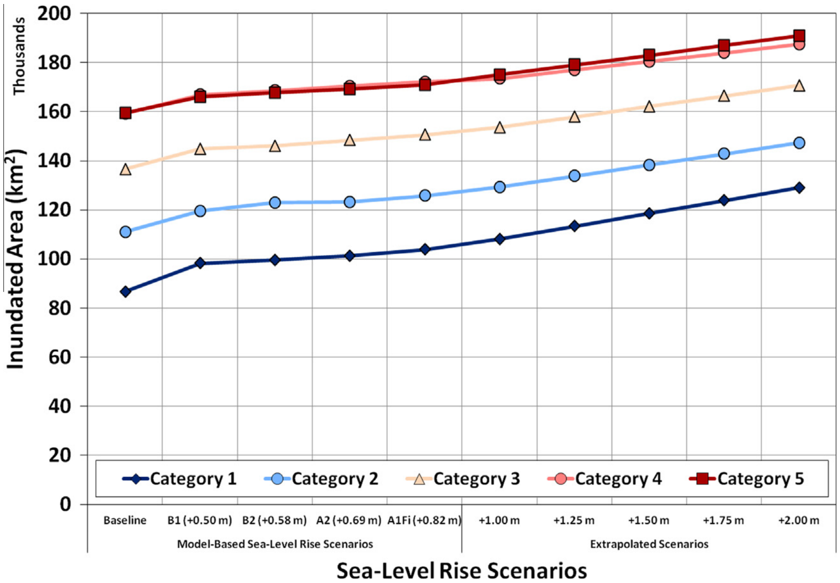

Fig. 2. Estimated U.S. coastal land area that could be exposed to inundation in response to storm surge associated with different Saffir-Simpson hurricane categories as well as different sea-level rise scenarios. The SRES sea-level rise scenarios were directly integrated with SLOSH model MOMs in the development of hazard layers while results for the extrapolated scenarios were based upon least-squares linear regression extensions of the SRES results.

accounting for such high magnitudes of sea-level rise, the coefficients of variation in land area exposed to storm surge inundation among different hurricane intensities (ranging from 24% assuming no sea-level rise to 16% assuming 2 m of sea-level rise) were greater than those among different 21st century sea-level rise scenarios (ranging from 12% for category 1 storms to 6% for category 5). Hence, potential changes in hurricane intensity (e.g., wind speed or central pressure) (Seneviratne et al., 2012) may be a greater concern for coastal exposure and vulnerability than sea-level rise.

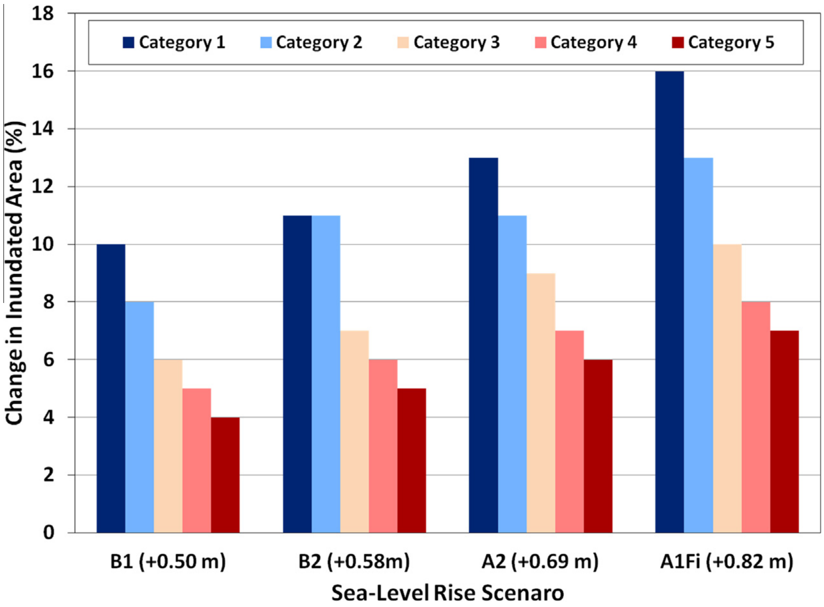

Fig. 3. Estimated percent changes in U.S. coastal land area exposed to storm surge inundation for different Saffir-Simpson hurricane categories and sea-level rise scenarios relative to results generated by the base case that assumes no change in sea level.

As suggested by previous studies (Frazier et al., 2010), the effects of future sea-level rise on storm surge inundation were comparable to increasing the magnitude of a hurricane to which a coastline is exposed, although this conclusion may be contingent upon the selected storm surge model and elevation data used in the current study. For example, the land area associated with hazard zones for category 1–3 storms using the A1Fi sea-level rise scenario (+0.82 m) were closer to the next higher base case Saffir-Simpson category (i.e., category 2–4 storms) than the original base case. This is consistent with a range of prior studies that have identified sea-level rise as a factor contributing to reductions in the annual return interval for storm surge levels (Lowe and Gregory, 2005; Claudia et al., 2012; Lin et al., 2012; Grinsted et al., 2013). However, as suggested by the extrapolated scenarios (Fig. 2), it would take significantly higher sea-level rise than the SRES scenarios used here for a lower intensity storm category and sea-level rise to result in a hazard zone equivalent to a higher intensity base case storm. Sea-level rise in 2100 would have to be 1.25–1.50 m in order for future category 1–3 hazard zones to meet or exceed current category 2–4 hazard zones. Such magnitudes of sea-level rise cannot, however, be ruled out (Pfeffer et al., 2008).

When disaggregated to the state level, inundation areas reflect a significant degree of heterogeneity among states with respect to both the magnitude of land subject to inundation as well as the sensitivity of inundation to sea-level rise. The majority of land area subject to inundation was accounted for by two states: Florida and Louisiana (Fig. 4). For example, given the base case hazard zone for category 3 storms, these two states accounted for approximately 55% of the total land area subject to inundation, followed by Texas and North Carolina, which captured another 28% of the total. Assuming sea-level rise equivalent to the A1Fi scenario (+0.82 m), the land area subject to inundation increased by an average of 11% among states, ranging from a 4% increase for Louisiana to a 17% increase for South Carolina. On an absolute basis, those states with the largest increase in category 3 hazard zones with sea-level rise included Florida (+5391 km^2), Texas (+1844 km^2), North Carolina (+1618 km^2), Louisiana (+1417 km^2), and South Carolina (+1147 km^2).

Case study applications

To illustrate potential applications of the geospatial storm surge hazard layers for first pass coastal assessment, two case studies are explored that use the hazard layers as a basis for assessing potential exposure of human systems and assets to storm surge and sea-level rise. The first focuses on the exposure of electricity generation facilities and oil refineries in the U.S. Southeast to storm surge inundation with and without sea-level rise. The second focuses on the exposure of residential housing adjacent to both the Gulf and Atlantic coasts. For each of these case studies, detailed information is available regarding the distribution of exposed assets, thereby maximizing the utility of high-resolution inundation information. The two case studies differ in their assumptions regarding future changes in the built environment. While reliable location estimates for existing energy infrastructure are readily available, scenarios that represent future expansion and/or their redistribution in response to changing energy demand, technologies, and risk are not. In contrast, the recent emergence of high resolution housing scenarios for the United States (Bierwagen et al., 2010) enable the consideration of changes in both biophysical

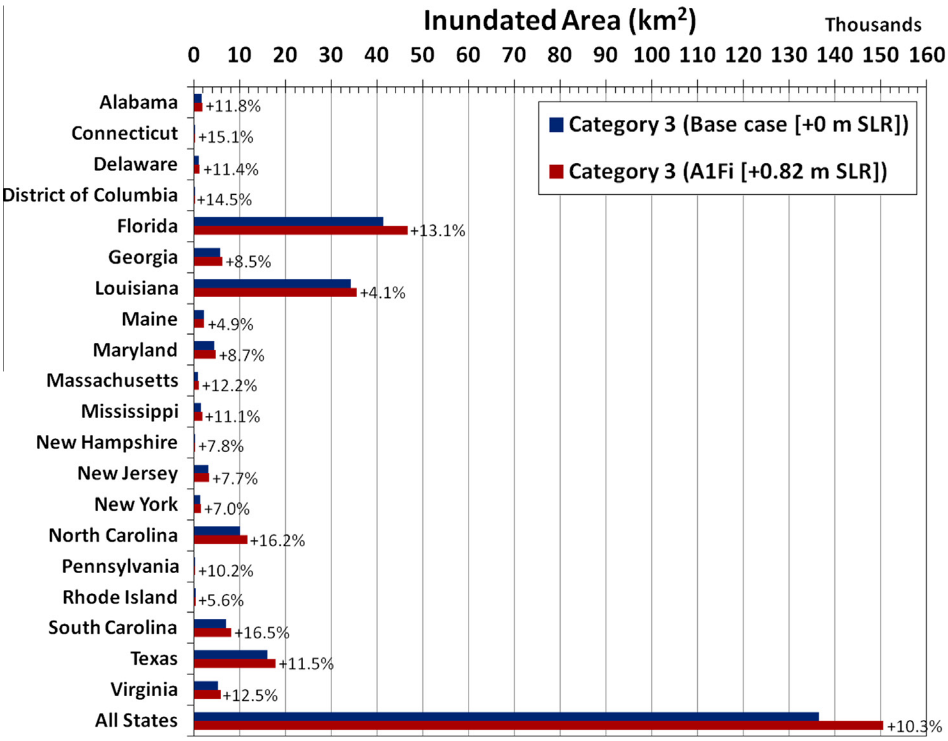

Fig. 4. Comparison of the estimated area within each state adjacent to the U.S. Gulf of Mexico or Atlantic Ocean that is exposed to inundation from category 3 hurricanes given a base case with no change in sea level and a sea-level rise scenario (A1Fi; +0.82 m by 2100).

factors such as sea-level rise and storm surge as well as socioeconomic conditions such as population growth and development. This also enables one to compare the relative contribution of sea-level rise and population growth to future societal exposure.

Case study 1: U.S. Southeast energy infrastructure

Locations of energy facilities in the 10 state U.S. Southeast region were identified through a geospatial database comprised of thermoelectric power plants, hydropower facilitates, renewable energy facilities, and oil refineries (Fig. 5). The dataset was provided by Oak Ridge National Laboratory and represents the results of a collaboration involving Oak Ridge National Laboratory (ORNL), Idaho National Laboratory (INL), and Argonne National Laboratory (ANL) to develop an energy infrastructure database as part of the Homeland Security Infrastructure Protection (HSIP) Freedom database accessible through the Homeland Security Information Network. The HSIP Freedom database is analogous to the HSIP Gold database, but with increased shareability within the Federal, State, and Local emergency response communities. The database was developed using open source information including digitized published open source, unrestricted reports; Federal Energy Regulatory Commission (FERC) filings openly published with unlimited distribution; remote sensing imagery; and datasets contributed by the various collaborating national laboratories. This dataset indicates that 1711 electricity generation facilities are located in the 10 state southeast region, with the three most common fuel types being natural gas, hydropower, and other renewables. Net operating capacity among these facilities was largely attributed to natural gas, coal, or nuclear plants. In addition, the database contained 54 oil refineries, which were concentrated in Texas and Louisiana, as well as the refining capacity of those facilities (Fig. 5). The dataset included facilities that have been decommissioned as well as those that have been planned but are not yet generating; both were included in the case study as former facilities have potential to be used in the future through redevelopment and repowering of the existing site, while the latter may be exposed to future climate change once operations commence. The majority of these facilities were adjacent to the Gulf of Mexico, which has been described as the 'Energy Coast' (America's Energy Coast, America's Wetlands Foundation, Entergy Corporation, 2008), and which has been the focus of prior energy infrastructure vulnerability assessments (Needham et al., 2012; Strauss and Ziemlinski, 2012).

Locations of power plants and oil refineries were intersected with each of the 25 storm surge hazard layers described previously in order to identify facilities that are potentially vulnerable to exposure to hurricane storm surge at present as well as with additional sea-level rise. As this analysis did not consider the depth of inundation and may not account for local structural defenses to protect infrastructure, those facilities that were identified were interpreted as being potentially exposed. No assumptions were made about subsequent impacts to exposed facilities as such a determination cannot be made based

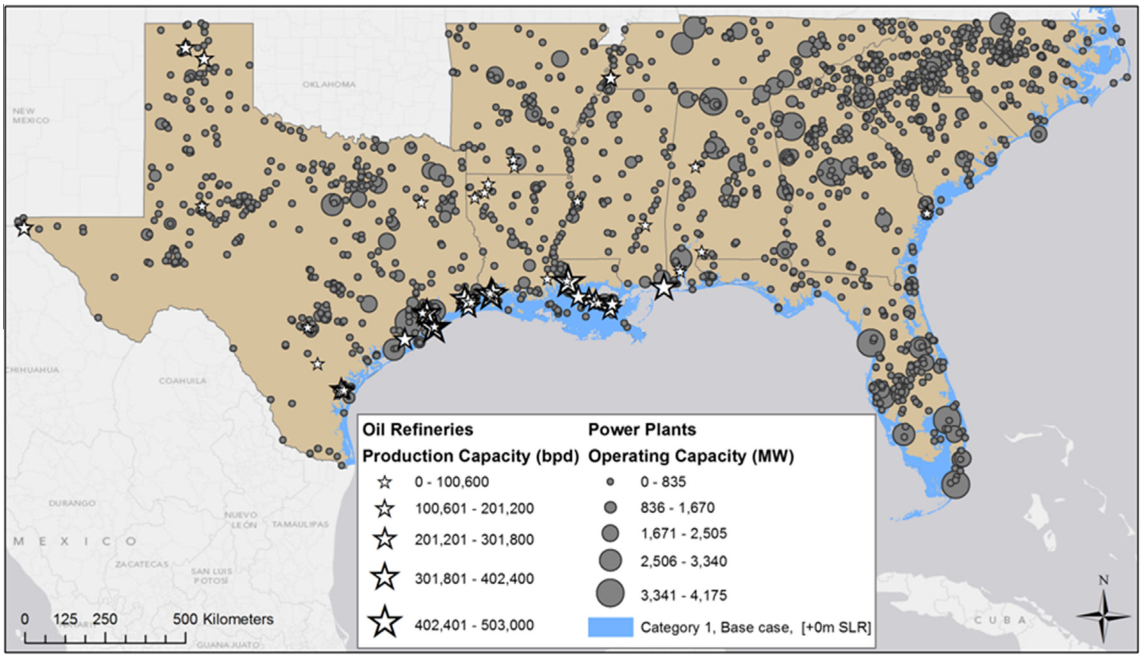

Fig. 5. Geographic distribution of electricity generation facilities and oil refineries in the ten state U.S. Southeast region as well as the coastal area potentially exposed to inundation from current category 1 storm.

upon exposure alone. However, prior events such as Gulf Coast hurricanes in 2005 and 2008 resulted in significant adverse impacts on energy infrastructure. During Hurricane Katrina, this included extensive flooding of power plants and oil refineries (NIST, 2006; DOE, 2009). Hence, exposure is a useful first-order proxy for adverse impacts, although more refined analysis would be needed for confident determination of risk at the scale of a specific site or facility (Murdukhayeva et al., 2013).

Of the 1711 electricity generating facilities in the database, the number currently vulnerable to storm surge inundation ranges from 69 for category 1 events to 291 for category 5 events (Fig. 6). The category 2 inundation zone doubled the number of exposed facilities compared to category 1, although the additional exposure associated with progressively larger storms diminished substantially. For example, the exposure associated with category 5 storms was just 13% higher than for category 4 storms. Sea-level rise significantly increased the number of vulnerable facilities, although the effect was particularly pronounced for hazard zones associated with category 1 and 2 storms. For example, just 0.5 m of sea-level rise increased the number of facilities vulnerable to a category 1 storm surge by 41%. For a category 3 storm, the increase was 8%, and just 5% for a category 5 storm. Similarly, additional increases in sea-level rise based on the A1Fi scenario contributed to a 60% increase in the number of exposed facilities for category 1 storms and just a 6% increase for category 5 storms. This nominal increase in exposure associated with sea-level rise highlights the existing exposure of infrastructure regardless of the relatively small additional burden related to future sea-level rise.

Exposure was also examined in terms of the electricity generation capacity of facilities. The increased exposure due to increasing hurricane intensities translated into exposure of total operating capacity in increasing steps of approximately 20,000 MW between the first four Saffir-Simpson categories (Fig. 6). There was less increase between categories four and five, perhaps due to increasing topography inland that impeded storm surge, high capacity facilities being grouped to serve vulnerable port cities (e.g., the 2100 base case category 5 hazard zone exposes 21% of total MW output capacity on just 8% of the land for the southeast study region), or facility placement that takes advantage of water features that provide cooling services. Of the 116 facilities in the region with an operating capacity above 1000 megawatts, five were located in the base case category 1 hazard zone, totaling 11,206 MW. Twenty eight were located in the base case category 5 hazard zone, totaling 52,597 MW; 24% of the total MW produced by >1000 MW capacity facilities in the region on 8% of the total land area. The maximum sea-level rise scenario, A1Fi, exposed one additional plant, bringing the total exposed operating capacity to 54,307 MW.

Although the number of oil refineries identified in the Southeast was significantly less than the number of power plants, a much larger fraction (61%) of oil refineries in the region were in coastal areas potentially exposed at present to storm surge inundation. Assuming no increase in sea-level rise, the number of exposed oil refineries ranged from 7 for category 1 storms to 33 for category 5 storms (Fig. 6). Consistent with results for power plants, while sea-level rise increased the number of facilities potentially exposed to storm surge inundation, this increase was most pronounced for low intensity hurricanes (i.e., category 1 and 2 on the Saffir-Simpson scale). For category 1 storms, the B1 (+0.50 m) sea-level rise scenario doubled the number of exposed facilities, but additional increases in sea level beyond this magnitude did not result in additional

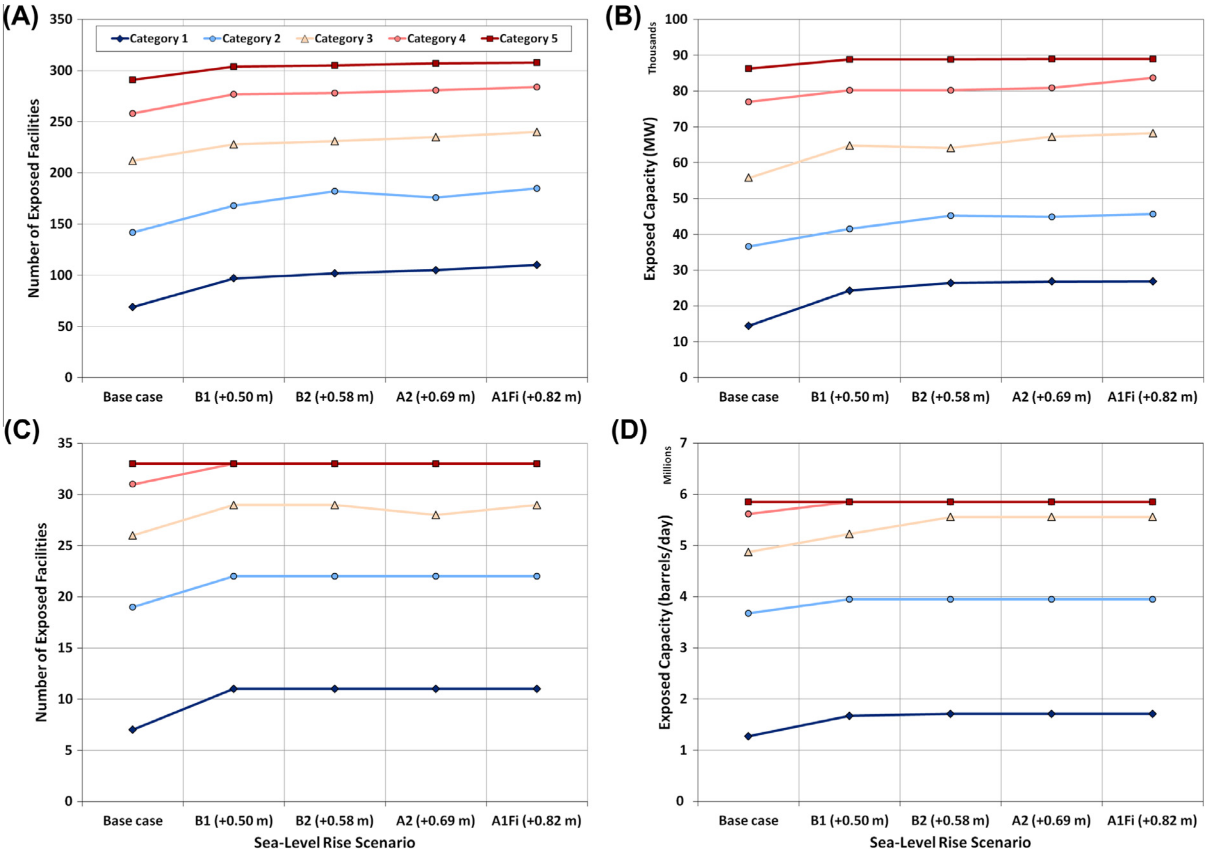

Fig. 6. Estimates of U.S. Southeast energy facilities that are potentially exposed to storm surge inundation and sea-level rise: (A) number of exposed electricity generating facilities; (B) megawatts of exposed electricity generation; (C) number of exposed oil refineries; (D) exposed oil production in barrels per day.

exposure. This relative insensitivity to higher magnitudes of sea-level rise was true for storms of all Saffir-Simpson categories except category 3 storms, for which the B2, A2, and A1Fi scenarios (+0.58–0.82 m) resulted in the exposure of one additional refining facility relative to the B1 scenario.

Again, given the refining capacity of different facilities varies, exposure was also explored in the context of the exposed refining capacity represented by vulnerable facilities. At present, facilities vulnerable to category 1 and category 5 storm surges represent 1.2 and 5.8 million barrels per day, respectively, of refining capacity (Fig. 6). The upper end of this range represents 74% of the total Southeast capacity, which further highlights this disproportionate concentration of refining facilities in the coastal zone. However, the response of exposure to greater storm intensities was similar to that for facility counts. The exposed refining capacity for category 2 storms was approximately 3 times that for category 1 storms. While higher magnitude storms contributed to further increases in exposed refining capacity these increases declined substantially as storms moved up the Saffir-Simpson scale. This indicates that the majority of refining capacity (63%) is concentrated in areas vulnerable to category 1 and 2 storms. As was observed with facility counts, exposed refining capacity was relatively insensitive to sea-level rise scenarios. For category 1 storms, the various sea-level rise scenarios increased the exposure of refining capacity by 30-34%. For category 2 and 3 storms, the increases were 7–14%, declining to 4% and 0% for category 4 and 5 storms, respectively.

Case study 2: U.S. residential housing

The geographic distribution of residential housing in U.S. coastal areas was based upon the Integrated Climate and Land Use Scenarios (ICLUS) developed for the EPA's Global Change Research Program in the Office of Research and Development's National Center for Environmental Assessment (Bierwagen et al., 2010). The ICLUS scenarios represent county population as well as gridded housing density and impervious surface estimates at resolutions of 0.01 and 1 km^2, respectively. In addition to representing current (i.e., 2005) estimates of population, housing density, and impervious surface, the ICLUS scenarios are also comprised of spatially explicit projections throughout the 21st century that are based upon the SRES socioeconomic scenarios (Nakicenovic et al., 2000). This includes the B1, B2, A1, and A2 families as well as a base case scenario that represented an intermediate development pathway (Bierwagen et al., 2010). The projections were created by the Spatially Explicit Regional Growth Model (SERGoM), which assesses changes in land cover classes and environmental variables at 0.01 km^2 resolution based on housing density growth patterns (Bierwagen et al., 2010). The SERGoM model uses population projections to allocate housing units in 5-year time steps. At each time step, the model uses the spatial pattern developed from the previous time step to guide the allocation of additional housing units. For the current study, ICLUS housing density values were extracted from each of the SRES scenarios for those areas that overlapped with the 25 hazard zone inundation polygons representing storm surge and/or sea-level rise.

To maintain internal consistency in assessing the exposure of housing to future storm surge and sea-level rise, storm surge hazard layers associated with a particular SRES scenario were used to extract data from the matching ICLUS housing density scenario. For example, ICLUS B1 housing density data were extracted for the SLOSH inundation zones calculated for the B1 sea-level rise estimate, and the ICLUS A1 scenario was paired with the SLOSH A1Fi inundation zones. For analyses that assumed current sea level, the ICLUS base case scenario was used. As with the sea-level rise scenarios, no assumption was made with respect to the absolute or relative likelihood of the housing density scenarios. To evaluate the components of change in future housing exposure, exposure was divided into four sources (Table 1): (a) current exposure, calculated from current hazard zones and housing, which was affected by neither sea-level rise, nor socioeconomic development; (b) future exposure solely attributable to sea-level rise, calculated using future hazard zones with current housing; (c) future exposure solely attributable to socioeconomic change, calculated using the housing growth within current hazard zones; and (d) future exposure attributable solely to combined drivers of sea-level rise and housing growth, calculated from the housing development occurring only in the additional land exposed by inundation associated with sea-level rise.

This methodology indicated that at present, exposure of housing units to storm surge inundation ranges from 4.1 million units for category 1 storms to 9.4 million for category 4 storms (Fig. 7). Potential exposure to category 5 storms is 7.1 million due to the absence of category 5 hurricanes and therefore MOM data in the Northeast. By using both the hazard layers accounting for sea-level rise and the ICLUS scenarios of future housing density, our analysis enabled the assessment of the net implications of these processes as well as their marginal contributions to future housing exposure (Fig. 7). When both factors were considered, the number of housing units projected to be exposed to storm surge inundation generally triples. However, as noted previously, the effects were more pronounced for storms at the bottom end of the Saffir-Simpson scale. For example, the number of housing units exposed to a category 1 storm increased from 4.1 million in 2005 to 10.7 million (+161%) assuming a B1 socioeconomic future and 13.5 million (+229%) assuming an A2 future which assumes higher population growth. In contrast, for a category 4 storm, exposure grew from 9.4 million in 2005 to 20.0 million (+113%) and 24.8 million (+164%) in 2100 for the B1 and A2 futures, respectively. It should be noted that while the A1Fi scenario assumes the largest increase in sea-level rise, the A2 scenario assumes the largest increase in population and housing. As a consequence, the A2 future results in the greatest increase in housing exposure by 2100.

At a sub-national level, housing exposure to storm surge and sea-level rise was heterogeneously distributed among coastal states. Of the approximately 21.4 million housing units potentially exposed to storm surge inundation from a category 3 event for an A2 scenario by 2100, just under half occurred in the state of Florida (Fig. 8). This was a function of Florida accounting for a significant fraction (31%) of U.S. land area that is exposed, as well as the high future growth in housing in the state. Approximately 51% of the net increase in housing in exposed areas between 2005 and 2100, for example, was projected to occur in Florida. In contrast, while Louisiana was associated with 31% of the total increase in land area exposed to a category 3 storm surge in 2100, it only accounted for 3% of the net increase in exposed housing. To further explore the attribution of exposure to different factors at the state level, the ratio of the percent change in socioeconomic (i.e., housing) exposure to category 3 storms from 2005 to 2100 for the A1Fi scenario to the percent change in land area exposed for the same scenario was calculated (Fig. 9). The results indicated that all states are expected to experience increases in housing exposure that are disproportionately large relative to the change in land area exposed to inundation. These ratios varied significantly among states, however. For Connecticut and Massachusetts, housing exposure was expected to grow at just twice the rate of growth in land exposure. At the opposite extreme, however, housing exposure in New York under the A1 scenario was projected to grow at a rate 39 times that of land exposure. These ratios would be ever larger under an A2 scenario, which has lower rates of sea-level rise, but higher rates of housing development.

These results indicate that despite significant discussion in the literature regarding the additional risks posed by climate change and sea-level rise to coastal communities and assets (Keim et al., 2007; Tebaldi et al., 2012), the change in future

Table 1

Decomposition of components of future changes in housing exposed to hurricane storm surge. Changes in housing exposure can arise from two factors: (a) sea-level rise that increases the land area exposed to inundation and/or (b) increases in housing on land exposed to inundation. The analysis reported here explores all permutations of these factors for each Saffir-Simpson category and SRES scenario (Fig. 7). The sum of all four components represents the projected exposure of housing in 2100.

Housing scenario	Sea-level rise scenario	
	Current	Future
Current	Current: Base case inundation area and current (2005) housing	SLR only: Inundation area associated with future sea-level rise and current (2005) housing
Future	Housing growth only: Base case inundation area and future (2100) housing	Housing growth and SLR: Additional inundation area due to sea-level rise (i.e., 2100 inundation area minus current) and future (2100) housing

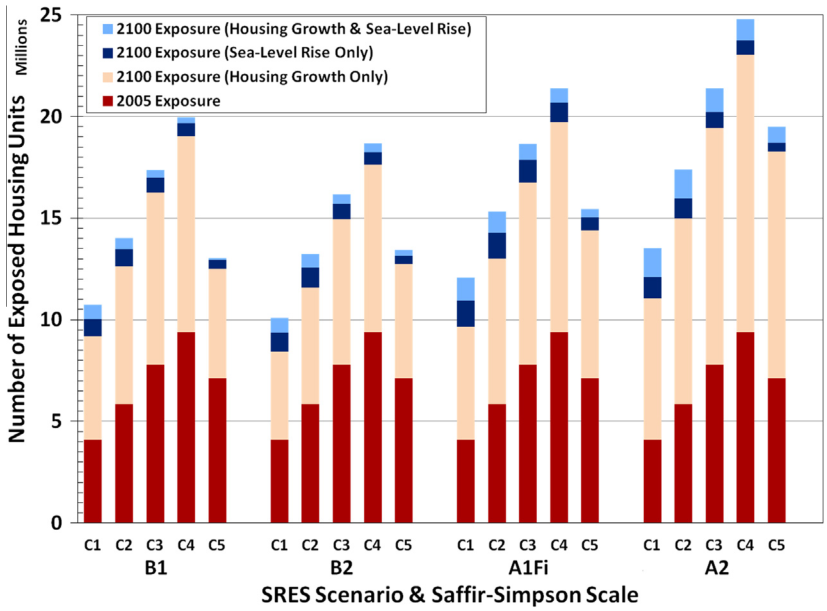

Fig. 7. Total number of housing units on the U.S. Gulf of Mexico and Atlantic coasts that are projected to be exposed to storm surge inundation by the year 2100. Housing unit exposure is disaggregated into current (i.e., 2005) exposure for each Saffir-Simpson hurricane category (C1–C5) as well as the components of future change associated with sea-level rise, increased housing development, and the interaction between the two (Table 1).

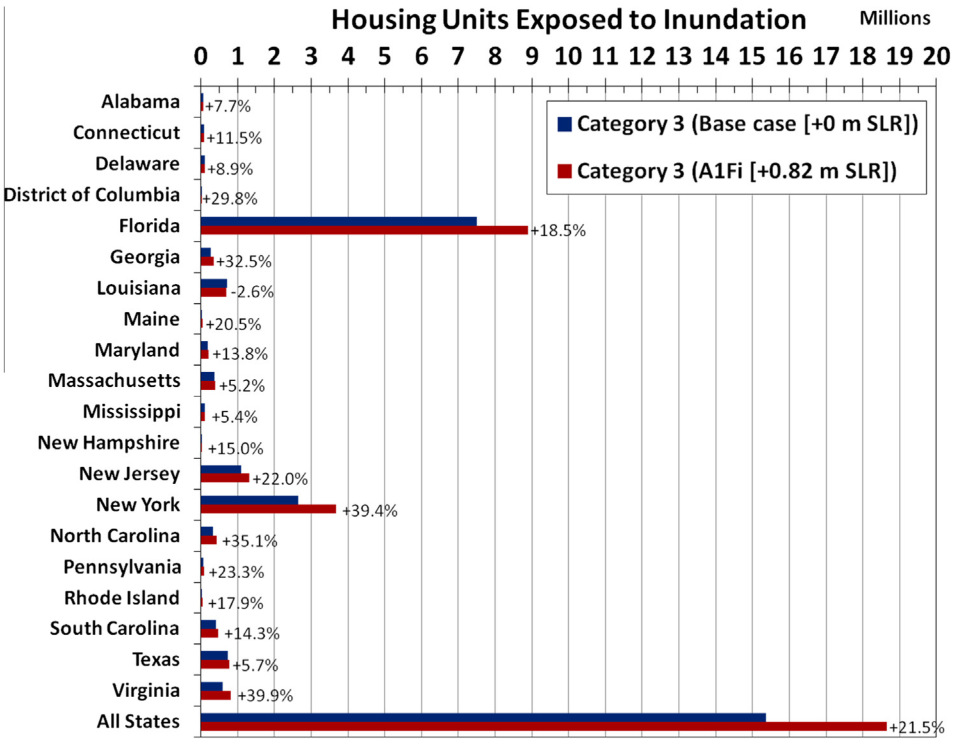

Fig. 8. Comparison of the number of housing units within each state adjacent to the Gulf of Mexico or Atlantic Ocean that are projected to be vulnerable to inundation from category 3 hurricanes by 2100 given a base case scenario with growth in housing but no sea-level rise and a scenario with both housing growth and sea-level rise (A1Fi; +0.82 m by 2100).

exposure largely will be dictated by socioeconomic trends that are projected to greatly expand the concentration of physical assets within hazardous coastal landscapes (Preston, 2013). Sea-level rise alone, for example, contributed to relatively small increases in housing exposure by increasing the land area potentially exposed to storm-surge inundation, and this increase

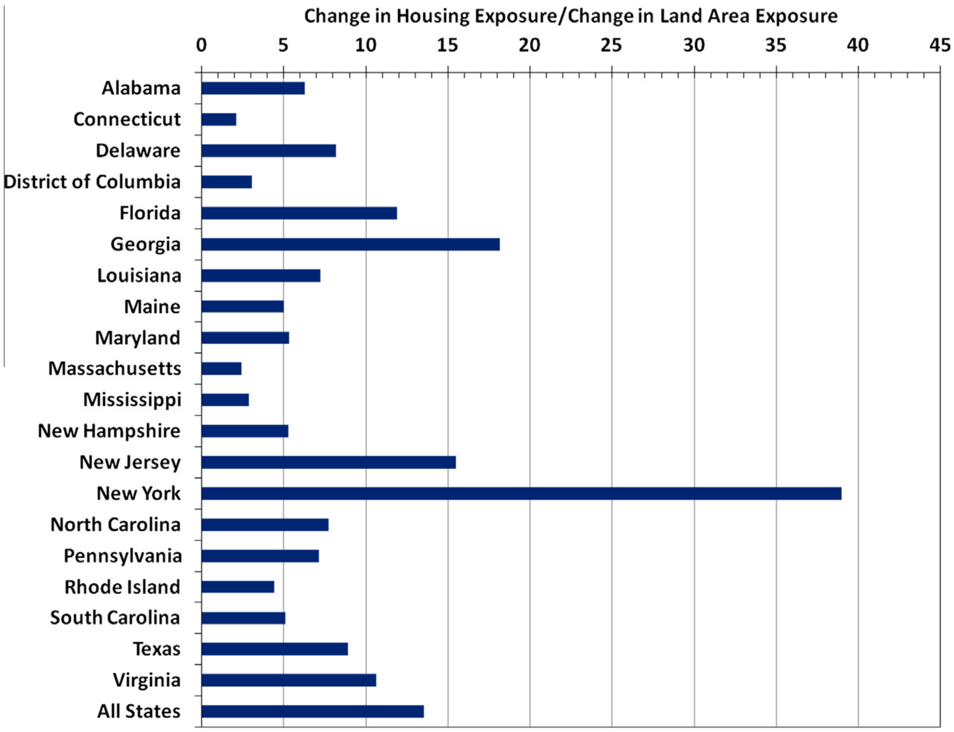

Fig. 9. Ratio of projected percentage change in housing exposed to a category 3 storm surge by the year 2100 (assuming a A1Fi sea-level rise scenario of +0.82 m) to the projected percentage change in land area exposed to a category 3 storm surge for states adjacent to the U.S. Gulf of Mexico and Atlantic coasts.

was most pronounced for the lowest intensity storms. In contrast, increases in future housing alone contributed to approximately a doubling of housing exposure by the end of the century. Nevertheless, consideration of the interactions between sea-level rise, storm surge, and future socioeconomic development are necessary for risk management.

Discussion

Future global and regional sea-level rise have been identified as a robust consequence of anthropogenic climate change, despite persistent challenges in constraining future estimates of the magnitude of sea-level rise (Rahmstorf, 2007; Meehl et al., 2007; Pfeffer et al., 2008; Rahmstorf, 2010; Rahmstorf et al., 2012). As such, coastal exposure to sea-level rise has been a major focal area of climate change impacts, adaptation and vulnerability research (Preston et al., 2011). Such studies often make discrete choices regarding methods for understanding the physical exposure and vulnerability of the coastline, including empirical or process-based modeling; assessment for sea-level rise alone or in combination with storm surge; and consideration for sea level elevation or coastal inundation. Each of these choices leads toward sets of investigative tools and methods and carry trade-offs that may make them more or less appropriate for certain applications. For example, consideration for just the inundation associated with sea-level rise can greatly underestimate coastal hazards, exposure, and therefore vulnerability in high energy coastlines and/or those that experience significant tropical cyclone activity (Nicholls et al., 1999; Titus and Richman, 2001; Nicholls and Small, 2002; DCC, 2009; Nicholls et al., 2010; Nicholls and Cazenave, 2010; Tebaldi et al., 2012). Meanwhile, studies that focus on understanding return intervals for sea level elevations provide information on the frequency of hazards, but may not offer useful information on the direct consequences of exposure (Lowe and Gregory, 2005; Claudia et al., 2012; Lin et al., 2012; Grinsted et al., 2013). Process-based methods based upon hydrodynamic modeling may capture the complexity of coastal dynamics, but such complexity may create challenges for large-scale applications due to computational and cost constraints. This may result in a multitude of well-executed case studies that are nevertheless difficult to integrate into a large-scale, systemic understanding of coastal vulnerability. These trade-offs suggest the need for a range of analysis tools that can be adapted as needed to address particular questions.

To this end, models of intermediate complexity may be an effective strategy for capturing complexity and detail while still enabling analyses over expansive geographic scales. As demonstrated here, the SLOSH model is one such platform. Its reduced complexity enables rapid deployment and application by those with limited technical background, and it remains the principle analysis tool for coastal evaluation planning and other municipal disaster risk management planning, which suggests the presence of an established pathway into organizational decision-making. This flexibility and intermediate complexity enables SLOSH modeling information to be applied in assessment over quite expansive geographic areas, including comprehensive coverage of U.S. coastlines exposed to hurricane landfall. It therefore makes a useful platform for nationally-consistent assessment of coastal exposure and/or vulnerability at spatial scales sufficient to capture spatial heterogeneity with respect to coastal morphology and human settlement patterns. That said, the structure of SLOSH modeling around dozens of individual basins poses some challenges to the development of national, internally consistent results. Translating SLOSH MOMs into inundation areas for multiple hurricane categories and sea-level rise assumptions and then integrating those layers across multiple basins is labor and computationally intensive in a desktop GIS environment. Yet, as demonstrated here, once that investment has been made, the resulting geospatial information regarding inundation exposure can be used for a range of assessment tasks based upon internally consistent, if still incomplete, assumptions regarding physical processes.

As a model of intermediate complexity, SLOSH-based inundation estimates are subject to a range of uncertainties (Kettle, 2012). For example, they lack processes such as coastal accretion/recession, changes in near-shore bathymetry, wave height and run-up, river flow, rain flooding, and coastal biogeochemistry. Furthermore, the methodology used here assumes the effects of sea-level rise are additive – an assumption that has been critiqued in the literature (Zhang et al., 2013; Atkinson et al., 2013), and it does not account for regional variability in absolute or relative sea-level rise due to factors such as land subsidence. Additional uncertainties are introduced by the elevation data used to translate SLOSH MOMs into inundation overlays. The USGS NED 30 m data used in the current study are derived from best available data sources. However, data quality is not homogeneous across the entire U.S. coastline, and uncertainties in vertical accuracy are on the order of 2.44 m (Gesch, 2007), which is greater than the storm surge surface water elevation changes assumed by sea-level rise scenarios. Higher-resolution elevation data with significantly lower vertical errors has enabled improvements in coastal assessments, as multiple studies have noted the disparities between Light Detection And Ranging (LiDAR) and NED DEMs (Poulter and Halpin, 2008; Gesch, 2009). While LiDAR data are not currently available for the entire U.S. coastline, such data are available in a number of locations and could be used for more refined second or third pass assessments on a regional or local level. However, integrating such high resolution elevation data with SLOSH MOMs with horizontal resolutions that are coarser by two to three orders of magnitude may result in false precision. Lastly, as the current study was used to develop geospatial understanding of U.S. potential exposure to storm surge, it does not address the return interval of storm events along the U.S. coast, which is an important consideration for coastal vulnerability (Bender et al., 2010; Knutson et al., 2010; Mendelsohn et al., 2012). Collectively, these missing elements may result in underestimation of the potential impacts of future hurricanes and storm surge, and therefore SLOSH-based inundation maps are somewhat conservative. Hence, despite its widespread use in disaster risk management, applications with SLOSH may be restricted to those where there is value in first-order or first pass understanding of potential inundation and/or where one is interested in relationships among storm surge and other biophysical or socioeconomic processes.

Despite these uncertainties, the current study illustrates the potential utility in the use of SLOSH for spatially-explicit assessments of storm surge exposure over large-geographic areas. For example while various assessments have identified Gulf Coast energy infrastructure as vulnerable to hurricanes and sea-level rise (CCSP, 2007; DHS, 2011; Needham et al., 2012; Strauss and Ziemlinski, 2012; Wilbanks et al., 2012), few spatially explicit and quantitative analyses have been conducted. Our energy infrastructure exposure assessment is analogous to that conducted by Strauss and Ziemlinski (2012), yet rather than assuming exposure based upon arbitrary coastal elevation contours, the current study incorporates some of the processes that would determine the potential for different elevations to be affected by storm-surge and/or sea-level rise of different magnitudes. However, as this analysis did not account for future changes in the number, size, and locations of future energy infrastructure, it is highly questionable whether assumptions about exposure based upon estimates of sea-level rise in 2100 are relevant to current, and particularly future, infrastructure. Although technology upgrades, repowering, and investments in other infrastructure such as transmission lines and transportation networks allow energy infrastructure to be long-lived (Lempert et al., 2002), future development and siting of energy infrastructure along the Gulf Coast, for example, will likely consider the evolution of coastal hazards. Hence, development of scenarios and models that enable a range of energy futures to be explored for vulnerable areas may aid in better understanding of future exposure, vulnerability, and risk management.

In contrast with the energy infrastructure case study, the examination of housing exposure incorporates explicit assumptions regarding future trajectories of housing development in the coastal zone. In so doing, the case study provides a broader context for considering coastal exposure and illustrates the importance of human agency and socioeconomic processes in influencing future exposure. The results demonstrate, for example, that changes in societal exposure will be dominated by human agency at the local level with respect to development decisions, and thus failure to consider future socioeconomic conditions may lead to biased perceptions of the forces driving exposure and therefore vulnerability. This becomes evident when comparing the changes in exposed energy infrastructure and housing just for Gulf Coast states over the 21st century relative to the change in exposed land area. While the ratio of the percent change in exposed housing to exposed land area by 2100 for category 3 events under the A1 scenario was 14.0, the same ratio for energy generating facilities was just 1.4, in part because that analysis did not account for future expansion of the Gulf Coast energy system. Hence, while much attention has been given to the inland penetration of sea-level rise and storm surge in low-lying coastal areas, little attention has been paid to how future economic development of hazardous landscapes could contribute to significant increases in societal exposure in future decades, despite comparatively small increases in the area subject to inundation. Preston (2013), for example, estimates that continued coastal development may cause economic losses from hurricanes to grow more quickly over the first half of the 21st century than the U.S. economy. Meanwhile, Schultz and Elliott (2013) find that natural disasters contribute to acceleration of development in affected areas, resulting in greater societal exposure to future disasters. These studies, in conjunction with the case studies reported here, emphasize that useful insights regarding future exposure, vulnerability, and risk in a changing climate are contingent upon integrated assessment that incorporates both physical hazards driven by climate change and socioeconomic exposure driven by economic and demographic change.

Conclusion

This paper has described the development of a set of geospatial data layers reflecting potential exposure to storm surge inundation and sea-level rise that can be used for first pass coastal assessments for the United States as well as more regionally focused second pass assessments. These data reveal the inequitable distribution of inundation risk across the eastern United States as well as the additional risk posed by sea-level rise through its interactions with storm surge. However, as demonstrated by the case study applications, exposure is strongly influenced by human agency with respect to siting of critical infrastructure and development of the built environment on what are potentially hazardous landscapes. A significant number of power plants and oil refineries are potentially exposed to coastal hazards along the U.S. 'Energy Coast', although the current study does not provide information on changes in the frequency of such inundation, and more precise methods are needed to evaluate exposure and vulnerability on a site-specific basis. Nevertheless, the locations of existing infrastructure represent a potential vulnerability to the U.S. energy system and future siting and investment decisions will have to accommodate the changing nature of coastal hazards and risk in future decades. Similarly, housing scenarios for the future suggest strong expansion of the built environment in areas that are exposed to storm surge inundation. While sea-level rise is a significant contributor to this increase in exposure for a number of states, for others, the effects of sea-level rise on the exposed land area are dwarfed by the effects of increased development in those areas. This highlights the importance of integrated approaches to assessment that incorporate the future dynamics of natural and human systems and, on a more practical level, suggests that human decision-making at regional to local scales will have a critical influence on future exposure to natural hazards, regardless of the future trajectory of climate change.

Acknowledgements

The authors acknowledge two different sources of funding. The development of the national storm surge dataset and its application in the coastal housing case study were sponsored through Oak Ridge National Laboratory's Laboratory Directed Research and Development Program. ORNL is managed by UT-Battelle, LLC, for the U.S. Department of Energy under contract DE-AC05-00OR22725. The energy infrastructure case study was sponsored by the U.S. Department of Energy, Office of Science, Biological and Environmental Research, Integrated Assessment Research Program. The authors also acknowledge the U.S. Geologic Survey for the use of the National Elevation Dataset as well as Steven Fernandez (ORNL) and Olufemi Omitaomu (ORNL) for providing the energy infrastructure data.

References

America's Energy Coast, America's Wetlands Foundation, Entergy Corporation, 2008. Building a Resilient Energy Gulf Coast: Executive Report 2008. Available from: <http://entergy.com/gulfcoastadaptation/>.
Atkinson, J., McKee Smith, J., Bender, C., 2013. Sea-level rise effects on storm surge and nearshore waves on the Texas coast: influence of landscape and storm characteristics. J. Waterway Port Coast. Ocean Eng. 139 (2), 98–117.
Aubrey, D.G., Emery, K.O., 1983. Eigenanalysis of recent United States sea levels. Cont. Shelf Res. 2 (1), 21–33.
Bender, M.A. et al, 2010. Modeled impact of anthropogenic warming on the frequency of intense Atlantic hurricanes. Science 327 (5964), 454–458.
Bierwagen, B.G. et al, 2010. National housing and impervious surface scenarios for integrated climate impact assessments. Proc. Natl. Acad. Sci. U.S.A. 107 (49), 20887–20892.
Boruff, B.J., Emrich, C., Cutter, S.L., 2005. Erosion hazard vulnerability of US coastal counties. J. Coastal Res., 932–942.
Burkett, V.R., Davidson, M.A. (Eds.), 2012. Coastal impacts, adaptation and vulnerability. A Technical Input to the 2012 National Climate Assessment. Cooperative Report to the 2013 National Climate Assessment. Island Press, Washington, DC.
CCSP, 2007. Effects of climate change on energy production and use in the United States. In: Wilbanks, T.J. et al. (Eds.), A Report by the U.S. Climate Change Science Program and the Subcommittee on Global Change Research. Department of Energy, Office of Biological & Environmental Research, Washington, DC.
Changnon, S.A., Easterling, D.R., 2000. Disaster management – US policies pertaining to weather and climate extremes. Science 289 (5487), 2053.
Church, J.A. et al, 2004. Estimates of the regional distribution of sea level rise over the 1950–2000 period. J. Clim. 17 (13), 2609–2625.
Cigler, B., 2009. Post-Katrina hazard mitigation on the Gulf coast. Public Organ. Rev. 9 (4), 325–341.
Claudia, T., Benjamin, H.S., Chris, E.Z., 2012. Modelling sea level rise impacts on storm surges along US coasts. Environ. Res. Lett. 7 (1), 014032.
Crowell, M. et al, 2010. An estimate of the US population living in 100-year coastal flood hazard areas. J. Coastal Res., 201–211.
Cutter, S.L., Emrich, C., 2005. Are natural hazards and disaster losses in the U.S. increasing? Eos Trans. Am. Geophys. Union 86 (41), 381–389.
Cutter, S.L., Boruff, B.J., Shirley, W.L., 2003. Social vulnerability to environmental hazards. Soc. Sci. Q. 84 (2), 242–261.
DCC, 2009. Climate Change Risks to Australia's Coasts: A First Pass National Assessment. Depatment of Climate Change, Canberra.
DHS, 2011. Louisiana Highway 1/Port Fourchon Study. U.S. Department of Homeland Security, Washington, DC.
DOE, 2009. Comparing the Impacts of the 2005 and 2008 Hurricanes on U.S. Energy Infrastructure. Office of Electricity Delivery and Energy Reliability, U.S. Department of Energy, Washington, DC.
FEMAURSCOE, 2003. SLOSH Display Training. FEMA, URS and the U.S. Army Corps of Engineers, Washington, DC.
Frazier, T.G. et al, 2010. Influence of potential sea level rise on societal vulnerability to hurricane storm-surge hazards, Sarasota County, Florida. Appl. Geogr. 30 (4), 490–505.
Füssel, H.-M., 2007. Vulnerability: a generally applicable conceptual framework for climate change research. Global Environ. Change 17 (2), 155–167.
Gall, M. et al, 2011. The unsustainable trend of natural hazard losses in the United States. Sustainability 3 (11), 2157–2181.
Gehrels, W.R. et al, 2002. Rapid sea-level rise in the Gulf of Maine, USA, since AD 1800. Holocene 12 (4), 383–389.

Gesch, D.B., 2007. The national elevation dataset. In: Maune, D. (Ed.), Digital Elevation Model Technologies and Applications: The DEM Users Manual, second ed. American Society for Photogrammetry and Remote Sensing, Bethesda, Maryland, pp. 99–118.
Gesch, D.B., 2009. Analysis of lidar elevation data for improved identification and delineation of lands vulnerable to sea-level rise. J. Coastal Res., 49–58.
Gesch, D. et al, 2002. The national elevation dataset. Photogramm. Eng. Rem. S. 68 (1), 5–11.
Gilmer, B., Brenner, J., Sheets, J., 2012. Informing Conservation Planning Using Sea-level Rise and Storm Surge Impact Estimates in Saint Andrew and Choctawhatchee Bays, Florida. The Nature Conservancy, Corpus Christi, TX.
Grinsted, A., Moore, J.C., Jevrejeva, S., 2013. Projected Atlantic hurricane surge threat from rising temperatures. Proc. Natl. Acad. Sci. 110 (14), 5369–5373.
Gurley, K., Masters, F., 2011. Post-2004 Hurricane field survey of residential building performance. Nat. Hazards Rev. 12 (4), 177–183.
Gutierrez, B.T., Plant, N.G., Thieler, E.R., 2011. A Bayesian network to predict vulnerability to sea-level rise: data report. In: Data Series 2011-601. U.S. Geological Survey, Reston, Virginia.
Hammar-Klose, E., Thieler, E.R., 2001. Coastal vulnerability to sea-level rise: a preliminary database for the U.S. Atlantic, Pacific, and Gulf of Mexico Coasts. In: U.S. Geological Survey Digital Data Series – 68, U.S. Geological Survey, Washington, DC. Available from: <http://pubs.usgs.gov/dds/dds68/>.
Hoffman, R.N. et al, 2010. An estimate of increases in storm surge risk to property from sea level rise in the first half of the twenty-first century. Weather Clim. Soc. 2 (4), 271–293.
Houston, J.R., Dean, R.G., 2011. Sea-level acceleration based on US tide gauges and extensions of previous global-gauge analyses. J. Coastal Res. 27 (3), 409–417.
Hunter, J., 2010. Estimating sea-level extremes under conditions of uncertain sea-level rise. Clim. Change 99 (3–4), 331–350.
IPCC, 2001. Summary for policymakers. In: Houghton, J.T. et al. (Eds.), Climate Change 2001: The Scientific Basis. Contribution of Working Group I to the Third Assessment Report of the Intergovernmental Panel on Climate Change. Cambridge University Press, Cambridge, United Kingdom and New York, NY, USA.
IPCC, 2013. Summary for policymakers. In: Stocker, T.F. et al. (Eds.), Climate Change 2013: The Physical Science Basis. Contribution of Working Group I to the Fifth Assessment Report of the Intergovernmental Panel on Climate Change. Cambridge University Press, Cambridge, United Kingdom and New York, NY, USA.
Keim, B.D., Muller, R.A., Stone, G.W., 2007. Spatiotemporal patterns and return periods of tropical storm and hurricane strikes from Texas to Maine. J. Clim. 20 (14), 3498–3509.
Kemp, A.C. et al, 2011. Climate related sea-level variations over the past two millennia. Proc. Natl. Acad. Sci. 108 (27), 11017–11022.
Kettle, N.P., 2012. Exposing compounding uncertainties in sea level rise assessments. J. Coastal Res., 161–173.
Klein, R.J.T., Nicholls, R.J., 1999. Assessment of coastal vulnerability to climate change. Ambio 28 (2), 182–187.
Kleinosky, L.R., Yarnal, B., Fisher, A., 2007. Vulnerability of Hampton Roads, Virginia to storm-surge flooding and sea-level rise. Nat. Hazards 40 (1), 43–70.
Knutson, T.R. et al, 2010. Tropical cyclones and climate change. Nat. Geosci. 3 (3), 157–163.
Lempert, R.J. et al, 2002. Capital cycles and the timing of climate change policy. In: Policy Series. Pew Center on Global Climate Change, Arlington, VA.
Lin, N. et al, 2012. Physically based assessment of hurricane surge threat under climate change. Nat. Clim. Change 2 (6), 462–467.
Lowe, J.A., Gregory, J.M., 2005. The effects of climate change on storm surges around the United Kingdom. Philos. Trans. R. Soc. A Math. Phys. Eng. Sci. 2005 (363), 1313–1328.
Mahendra, R.S. et al, 2011. Assessment and management of coastal multi-hazard vulnerability along the Cuddalore-Villupuram, east coast of India using geospatial techniques. Ocean Coast. Manag. 54 (4), 302–311.
McInnes, K.L. et al, 2013. An assessment of current and future vulnerability to coastal inundation due to sea-level extremes in Victoria, southeast Australia. Int. J. Climatol. 33 (1), 33–47.
McLeod, E. et al, 2010. Sea-level rise impact models and environmental conservation: a review of models and their applications. Ocean Coast. Manag. 53 (9), 507–517.
Meehl, G.A. et al, 2007. Global climate projections. In: Solomon, S. et al. (Eds.), Climate Change 2007: The Physical Science Basis. Contribution of Working Group I to the Fourth Assessment Report of the Intergovernmental Panel on Climate Change. Cambridge University Press, Cambridge, United Kingdom and New York, NY, USA.
Mendelsohn, R. et al, 2012. The impact of climate change on global tropical cyclone damage. Nat. Clim. Change 2 (3), 205–209.
Murdukhayeva, A. et al, 2013. Assessment of inundation risk from sea level rise and storm surge in northeastern coastal national parks. J. Coastal Res.
Nakicenovic, N. et al., 2000. Special Report on Emissions Scenarios: A Special Report of Working Group III of the Intergovernmental Panel on Climate Change. Pacific Northwest National Laboratory, Richland, WA (US), Environmental Molecular Sciences Laboratory (US).
Needham, H., Brown, D., Carter, L., 2012. Impacts and adaptation options in the Gulf coast. In: Science. Center for Climate and Energy Solutions, Arlington, VA.
Nicholls, R.J., Cazenave, A., 2010. Sea-level rise and its impact on coastal zones. Science 328 (5985), 1517–1520.
Nicholls, R.J., Leatherman, S.P., 1996. Adapting to sea-level rise: relative sea-level trends to 2100 for the United States. Coastal Manag. 24 (4), 301–324.
Nicholls, R.J., Small, C., 2002. Improved estimates of coastal population and exposure to hazards released. Eos Trans. Am. Geophys. Union 83 (28), 301–305.
Nicholls, R.J. et al, 2010. Sea-level rise and its possible impacts given a 'beyond 4 C world' in the twenty-first century. Philos. Trans. R. Soc. A Math. Phys. Eng. Sci. 2011 (369), 161–181.
Nicholls, R.J., Hoozemans, F.M.J., Marchand, M., 1999. Increasing flood risk and wetland losses due to global sea-level rise: regional and global analyses. Global Environ. Change 9 (Suppl. 1), S69–S87.
NIST, 2006. Performance of Physical Structures in Hurricane Katrina and Rita: A Reconnaissance Report. National Institute of Standards and Technology, Gaithersburg, Maryland, USA, p. 222.
NWS, 2011. SLOSH Pages: Sea, Lake, and Overland Surge from Hurricanes. Available from: <http://www.nhc.noaa.gov/ssurge/ssurge_slosh.shtml#COVERAGE> (cited 2013 May 14).
Pfeffer, W.T., Harper, J., O'Neel, S., 2008. Kinematic constraints on glacier contributions to 21st-century sea-level rise. Science 321 (5894), 1340–1343.
Pielke, R.A., 1860. Future economic damage from tropical cyclones: sensitivities to societal and climate changes. Philos. Trans. R. Soc. A Math. Phys. Eng. Sci. 2007 (365), 2717–2729.
Poulter, B., Halpin, P.N., 2008. Raster modelling of coastal flooding from sea-level rise. Int. J. Geogr. Inf. Sci. 22 (2), 167–182.
Preston, B.L., 2013. Local path dependence of U.S. socioeconomic exposure to climate extremes and the vulnerability commitment. Global Environ. Change.
Preston, B.L. et al, 2009. Igniting change in local government: lessons learned from a bushfire vulnerability assessment. Mitig. Adapt. Strat. Glob. Change 14 (3), 251–283.
Preston, B.L., Yuen, E.J., Westaway, R.M., 2011. Putting vulnerability to climate change on the map: a review of approaches, benefits, and risks. Sustain. Sci. 6 (2), 177–202.
Preston, B.L., Dow, K., Berkhout, F., 2013. The climate adaptation frontier. Sustainability 5 (3), 1011–1035.
Rahmstorf, S., 2007. A semi-empirical approach to projecting future sea-level rise. Science 315 (5810), 368–370.
Rahmstorf, S., 2010. A new view on sea level rise. Nat. Rep. Clim. Change, 44–45.
Rahmstorf, S., Perrette, M., Vermeer, M., 2012. Testing the robustness of semi-empirical sea level projections. Clim. Dyn. 39 (3–4), 861–875.
Roemmich, D., 1992. Ocean warming and sea level rise along the southwest US coast. Science 257 (5068), 373–375.
Rygel, L., O'sullivan, D., Yarnal, B., 2006. A method for constructing a social vulnerability index: an application to hurricane storm surges in a developed country. Mitig. Adapt. Strat. Glob. Change 11 (3), 741–764.
Schultz, J., Elliott, J., 2013. Natural disasters and local demographic change in the United States. Popul. Environ. 34 (3), 293–312.
Seneviratne, S.I. et al, 2012. Changes in climate extremes and their impacts on the natural physical environment. In: Field, C.B., Barros, V., Stocker, T.F., Qin, D., Dokken, D.J., Ebi, K.L., Mastrandrea, M.D., Mach, K.J., Plattner, G.-K., Allen, S.K., Tignor, P.M.M.M. (Eds.), Managing the Risks of Extreme Events and

Disasters to Advance Climate Change Adaptation. A Special Report of Working Groups I and II of the Intergovernmental Panel on Climate Change (IPCC). Cambridge University Press, Cambridge, UK, pp. 109–230.
Sharples, C., Attwater, C., Carley, J., 2008. Three pass approach to coastal risk assessment. In: IPWEA National Conference on Climate Change ''Responding to Sea Level Rise''. IPWEA, Coffs Harbour, NSW, Australia.
Smit, B., Wandel, J., 2006. Adaptation, adaptive capacity and vulnerability. Global Environ. Change 16 (3), 282–292.
Strauss, B., Ziemlinski, R., 2012. Sea Level Rise Threats to Energy Infrastructure. Climate Central, Washington, DC.
Tebaldi, C., Strauss, B.H., Zervas, C.E., 2012. Modelling sea level rise impacts on storm surges along US coasts. Environ. Res. Lett. 7 (1), 014032.
Titus, J.G., Richman, C., 2001. Maps of lands vulnerable to sea level rise: modeled elevations along the US Atlantic and Gulf coasts. Clim. Res. 18 (3), 205–228.
Titus, J.G. et al, 2009. State and local governments plan for development of most land vulnerable to rising sea level along the US Atlantic coast. Environ. Res. Lett. 4 (4), 1–7.
Turner, B.L. et al, 2003a. A framework for vulnerability analysis in sustainability science. Proc. Natl. Acad. Sci. 100 (14), 8074–8079.
Turner, B.L. et al, 2003b. Illustrating the coupled human–environment system for vulnerability analysis: three case studies. Proc. Natl. Acad. Sci. 100 (14), 8080–8085.
US Army Corps of Engineers, FEMA, NOAA, Maryland Silver Jackets Partnership, 2011. Two Coastal Flood Inundation Maps – Which Should I Use? Hurricane Evacuations Study – Storm Surge Inundation Mapping vs. National Flood INsurance Program – Flood Insurance Rate Map. An Overview and Comparison. US Army Corps of Engineers, FEMA, NOAA, Maryland Silver Jackets Partnership. Available from: <http://stormsmart.org/wp-content/blogs.dir/1/files/group-documents/220/1340560050-CoastalFloodMaps_HurrEvacMaps_vs_FIRMs_Final_Dec2011.pdf>.
Vallee, D.R., 2000. A Centennial Review of Major Land-Falling Tropical Cyclones in Southern New England. Available from: <http://www.erh.noaa.gov/box/hurricane/tropicalCycloneReview.shtml> (cited 2013 May 15).
Van Der Vink, G. et al, 1998. Why the United States is becoming more vulnerable to natural disasters. Eos Trans. Am. Geophys. Union 79 (44), 533–537.
Voice, M., Harvey, N., Walsk, K., 2006. Vulnerability to climate change of Australia's coastal zone: analysis of gaps in methods, data and system thresholds. In: Adam, A. (Ed.), Report to the Australian Greenhouse Office. Australian Greenhouse Office, Department of Environment and Heritage, Canberra.
Wilbanks, T. et al, 2012. Climate change and energy supply and use. In: Technical Report for the U.S. Department of Energy in Support of the National Climate Assessment. Oak Ridge National Laboratory and U.S. Department of Energy, Oak Ridge, TN.
Yin, J. et al, 2012. National assessment of coastal vulnerability to sea-level rise for the Chinese coast. J. Coastal Conserv. 16 (1), 123–133.
Young, G.M., 2003. NGS geodetic tool kit, part I. Prof. Surveyor Mag. 23 (4), 1–2.
Zhang, K. et al, 2013. Comparison of three methods for estimating the sea level rise effect on storm surge flooding. Clim. Change 118 (2), 487–500.